Structural characterization of cationic DODAB bilayers containing C24:1 β-glucosylceramide

Letícia S. Martins[a], Daniela A. Nomura[b], Evandro L. Duarte[b], Karin A. Riske[a], M. Teresa Lamy[b], Julio H.K. Rozenfeld[a],*

[a] Departamento de Biofísica, Escola Paulista de Medicina, Universidade Federal de São Paulo, R. Botucatu 862, 04023-062 São Paulo, SP, Brazil
[b] Instituto de Física, Universidade de São Paulo, CP 66318, CEP 05315-970 São Paulo, SP, Brazil

ABSTRACT

The effect of 5 mol%, 9 mol%, and 16 mol% of C24:1 β-glucosylceramide (βGlcCer) on the structure of cationic DODAB bilayers was investigated by means of differential scanning calorimetry (DSC), electron spin resonance (ESR) spectroscopy and fluorescence microscopy. βGlcCer is completely miscible with DODAB at all fractions tested, since no domains were observed in fluorescence microscopy or ESR spectra. The latter showed that βGlcCer destabilized the gel phase of DODAB bilayers by decreasing the gel phase packing. As a consequence, βGlcCer induced a decrease in the phase transition temperature and cooperativity of DODAB bilayers, as seen in DSC thermograms. ESR spectra also showed that βGlcCer induced an increase in DODAB fluid phase order and/or rigidity. Despite their different structures, a similar effect of loosening the gel phase packing and turning the fluid phase more rigid/organized has also been observed when low molar fractions of cholesterol were incorporated in DODAB bilayers. The structural characterization of mixed membranes made of cationic lipids and glucosylceramides may be important for developing novel immunotherapeutic tools such as vaccine adjuvants.

1. Introduction

Glucosylceramides are widely distributed components of cell membranes that serve as precursors for the synthesis of complex glycosphingolipids and as key intracellular messengers [1,2]. They are involved in several physiological processes such as embryogenesis, energy homeostasis and apoptosis [1], as well as in pathological processes such as cancer and sphingolipidosis [3,4]. They also play a significant role in the regulation of immune responses [5,6]. It was shown, for instance, that the C24:1 β-glucosylceramide (βGlcCer; Fig. 1), which is abundant in detergent-insoluble membrane domains of multidrug resistant cancer cells [7], is able to activate macrophages in response to cell damage [8].

The structural characterization of membranes containing glucosylceramides has focused mainly on natural mixtures from plant [9], bovine brain [10] and tissue samples from Gaucher's disease patients [11,12], or in mixtures of synthetic glucosylceramides and phospholipids or sphingomyelin [13,14]. The use of pure samples has been restricted to synthetic short chain saturated glucosylceramides [14–16]. However, the diversity of experimental conditions and molecules employed, which complicates comparison of literature data [17], did not

contemplate the structural characterization of glucosylceramides embedded in cationic membranes.

Cationic membranes have been initially developed as nucleic acid carriers [18], but they were also shown to induce immune responses [19]. This is the case for dioctadecyldimethylammonium bromide (DODAB, Fig. 1) [20], a versatile lipid that has been successfully used as a vaccine adjuvant [21,22]. The combination of DODAB with other molecules that are able to stimulate immune responses, such as βGlcCer, could lead to the development of novel immunotherapeutic tools [23,24]. Indeed, mixtures of DODAB and trehalose 6,6′-dibehenate (TDB), a glycolipid derived from *Mycobacterium* cord factor, resulted in strong immune responses [25].

Hence, in the present work, cationic DODAB membranes prepared with 5 mol%, 9 mol%, and 16 mol% of C24:1 β-glucosylceramide were for the first time characterized by means of differential scanning calorimetry (DSC), electron spin resonance (ESR) spectroscopy and fluorescence microscopy.

---

* Corresponding author.
E-mail address: julio.rozenfeld@unifesp.br (J.H.K. Rozenfeld).
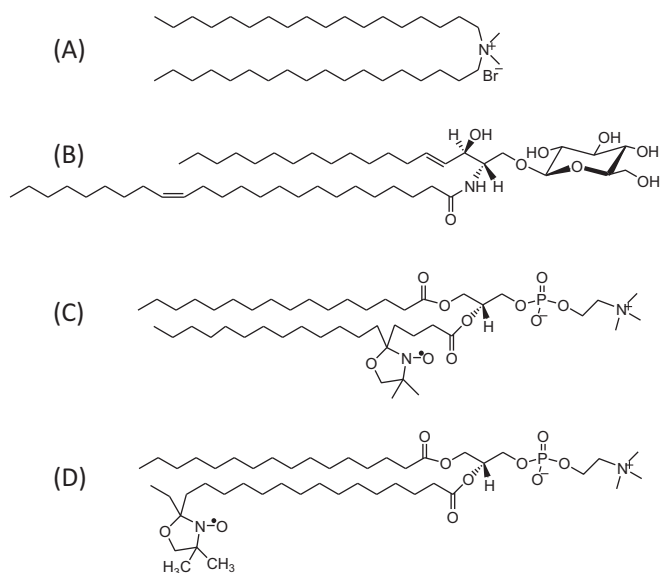
(A)

(B)

(C)

(D)

Fig. 1. Chemical structures of DODAB (A), βGlcCer (B), 5-PCSL (C) and 16-PCSL (D).

2. Materials and methods

2.1. Materials

Dioctadecyldimethylammonium bromide (DODAB), HEPES buffer, sucrose and glucose were purchased from Sigma Chemical Co. (St. Louis, MO, USA). D-glucosyl-β1–1′-N-nervonoyl-D-*erythro*-sphingosine (βGlcCer), spin labels 1-palmitoyl-2-(n-doxylstearoyl)-sn-glycero-3-phosphocholine (n-PCSL, n = 5 or 16) and the fluorescent probe 1,2-dipalmitoyl-sn-glycero-3-phosphoethanolamine-N-(lissamine rhodamine B sulfonyl) (ammonium salt) (PE-Rh) were supplied by Avanti Polar Lipids (Birmingham, AL, USA). Ultrapure water was used throughout. The chemical structures of DODAB, βGlcCer, 5- and 16-PCSL are shown in Fig. 1.

2.2. Liposome preparation

Lipid films of DODAB, βGlcCer, or DODAB plus βGlcCer were formed from a 2:1 (v/v) chloroform/methanol solution, dried under a stream of N$_2$, and left under reduced pressure for 2 h to remove all traces of organic solvent. Liposomes (large unilamellar vesicles) were prepared by adding HEPES buffer (10 mM, pH 7.4) to the films and heating them for 20 min at 80 °C. Heating was accompanied by vigorous vortexing at every 5 min in order to ensure a homogenous dispersion. For ESR experiments, 0.8 mol% 5-PCSL or 0.3 mol% 16-PCSL were added to the chloroform/methanol solutions when preparing the lipid films. No spin-spin interaction was observed at such small label concentrations. For fluorescence microscopy assays, 0.5 mol% PE-Rh were added to the chloroform/methanol solutions when preparing the lipid films and liposomes were made in HEPES buffer containing 200 mM sucrose. Final DODAB concentration was 2 mM. Final βGlcCer concentrations were 0.1 mM, 0.2 mM or 0.4 mM, which correspond, respectively, to 5 mol%, 9 mol%, and 16 mol% of the total lipid concentration.

2.3. Differential scanning calorimetry (DSC)

DSC scans were performed in a Microcal VP-DSC Microcalorimeter (Microcal Inc., Northampton, MA, USA) equipped with 0.5 mL twin total-fill cells. Heating rates were 5 °C/h. Scans were performed at least in duplicate. Thermograms correspond to second upscan.

2.4. ESR spectroscopy

ESR spectra were obtained with an X band Bruker EMX spectrometer using a high sensitivity ER4119HS cavity. The sample temperatures were controlled within 0.1 °C by a Bruker BVT-2000 variable temperature device. Empirical data correspond to the means of at least two experiments with standard deviations.

The effective order parameter, S_{eff}, was calculated from the expression [26,27].

$$S_{eff} = \frac{A_{//} - A_{\perp}}{A_{ZZ} - (1/2)(A_{xx} + A_{yy})} \frac{a_o{'}}{a_o}$$

where $a_o = (1/3)(A_{xx} + A_{yy} + A_{zz})$, $a_o = (1/3)(A_{//} + 2A_{\perp})$, $A_{//}$ (= Amax) is the maximum hyperfine splitting directly measured in the spectrum (see Fig. 6), $A_{\perp} = A_{min} + 1.4 \left[1 - \frac{A_{//} - A_{min}}{A_{zz} - (1/2)(A_{xx} + A_{yy})}\right]$, A_{min} is the measured inner hyperfine splitting (see Fig. 6) and A_{xx}, A_{yy} and A_{zz} are the principal values of the hyperfine tensor for doxylpropane [28]. The central field linewidth (ΔH_0) and the ratio between the high and central field line amplitudes (h_{-1}/h_0) were also taken directly from spectra (see Figs. 3 and 6).

2.5. Fluorescence microscopy

Liposomes prepared in 200 mM sucrose (item 2.2) were diluted 1:1 (v/v) in equiosmolar HEPES buffer containing 200 mM glucose to a final volume of 80 μL. After dilution, samples were centrifuged (2 min/13,000 rpm), giant liposomes were pelleted and 40 μL of supernatant were replaced by fresh buffer containing glucose. After supernatant replacement, giant liposomes (~10 μm) were carefully resuspended by pipetting. The centrifugation, supernatant replacement and liposome resuspension steps were repeated two more times in order to decrease fluorescence background effects by removing small liposomes. Additionally, this ensured a sugar asymmetry in the vesicles, which deposited on the coverslip due to the difference in density and increased the optical contrast in phase contrast mode. Liposomes were then transferred into an observation chamber connected to a water circulating bath that allowed temperature control [29]. The liposomes were observed with a Ph2 63× objective in an inverted Zeiss Axiovert 200 (Jena, Germany) equipped with a digital camera PCO.edge 4.2 (Kelheim, Germany) [29]. Illumination was achieved with an HBO 103 W mercury lamp and filters with excitation at 540–552 nm and emission band at 575–640 nm.

3. Results

3.1. βGlcCer decreases the transition temperature and cooperativity of DODAB bilayers

Thermograms of 2 mM DODAB, 0.2 mM βGlcCer and mixtures of 2 mM DODAB + βGlcCer are shown in Fig. 2. A very slow scan rate (5 °C/h) was employed in order to make sure that samples were in thermodynamic equilibrium.

In HEPES buffer, diluted DODAB dispersions show a single cooperative gel-fluid phase transition peaking at 47.1 °C, as previously described [30] (Fig. 2). On the other hand, βGlcCer displays an exothermic peak at 36 °C, a discrete endothermic peak at 45 °C and two more intense endothermic peaks at 57 °C and 66 °C (Fig. 2). A very similar thermogram profile was obtained for βGlcCer dispersions in water [31].

The mixed DODAB + βGlcCer bilayers show broader transitions that are shifted to smaller temperatures: the mixture with 0.1 mM βGlcCer has a peak at 45.7 °C and a shoulder at 41 °C; similarly, the mixture with 0.2 mM has a peak at 45.3 °C and shoulder at 41 °C. The mixture with 0.4 mM βGlcCer has several peaks, the most intense being at 39.3 °C (Fig. 2).
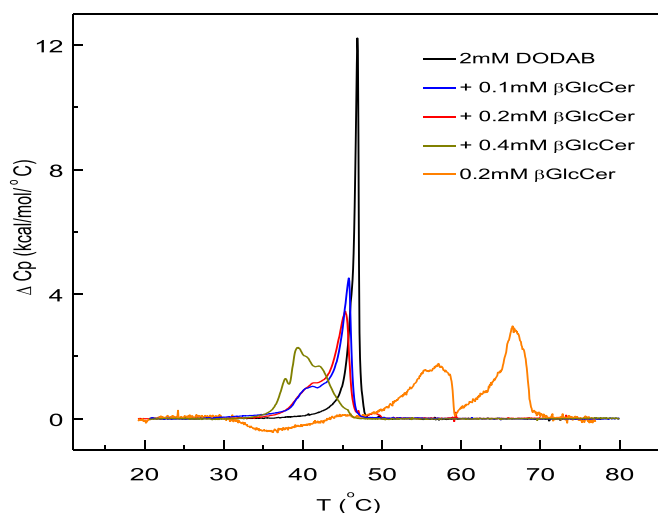
Fig. 2. Effect of βGlcCer on the DSC thermogram of 2 mM DODAB bilayers. Scan rate was 5 °C/h.

3.2. βGlcCer decreases the DODAB gel phase packing

The structure of pure DODAB and mixed DODAB + βGlcCer bilayers were compared by means of ESR spectroscopy, which probes the environment around the paramagnetic label attached to the phospholipid acyl chain [27,32]. For instance, 5-PCSL probes the bilayer close to the water interface, whereas 16-PCSL gives information about the bilayer core (Fig. 1). Spectra of 5- and 16-PCSL in pure and mixed membranes are shown for the temperature range of 20 °C–30 °C in Fig. 3.

In pure and mixed membranes, the spectra of both probes are typical of nitroxides in a tightly packed environment such as the gel phase (Fig. 3). However, the spectra of 5-PCSL are more anisotropic than the ones of 16-PCSL, showing that the membranes are less packed in the core than close to the surface, i.e., they exhibit a flexibility gradient toward the core [28].

The spectra of 5-PCSL in pure DODAB and mixed DODAB + βGlcCer membranes are similar. The same is observed for the spectra of 16-PCSL (Fig. 3). Empirical parameters obtained from ESR spectra can provide more details on membrane structure. In the gel phase an important parameter is the maximum hyperfine splitting (A_{max}), which is sensitive to the viscosity and packing of the environment surrounding the label [27]. In the cases where the A_{max} cannot be accurately measured, such as the 16-PCSL spectra shown in Fig. 3, the central field linewidth (ΔH_0) can be similarly employed. ΔH_0 becomes larger as the probe movement gets slower [28]. Fig. 4 shows the empirical parameters measured in the spectra of 5- and 16-PCSL embedded in the gel phase of pure and mixed bilayers.

The membrane packing decreases as temperature increases, so A_{max} and ΔH_0 values also decrease with temperature. A_{max} and ΔH_0 values are smaller for mixed DODAB + βGlcCer membranes than for pure DODAB membranes, showing that mixed vesicles are less packed at the core and near the surface than pure vesicles (Fig. 4).

3.3. βGlcCer affects DODAB bilayer organization around the gel-fluid transition

Spectra of 5- and 16-PCSL in a temperature range spanning the gel-fluid transition of pure and mixed membranes are shown in Fig. 5.

At 35 °C, the spectra of 5- and 16-PCSL in pure DODAB bilayers and in mixtures with 0.1 mM and 0.2 mM βGlcCer are typical of a tightly packed environment such as the gel phase (Fig. 5). On the other hand, in the mixture containing 0.4 mM βGlcCer it is possible to observe two signals in the same spectrum, which are characteristic of the
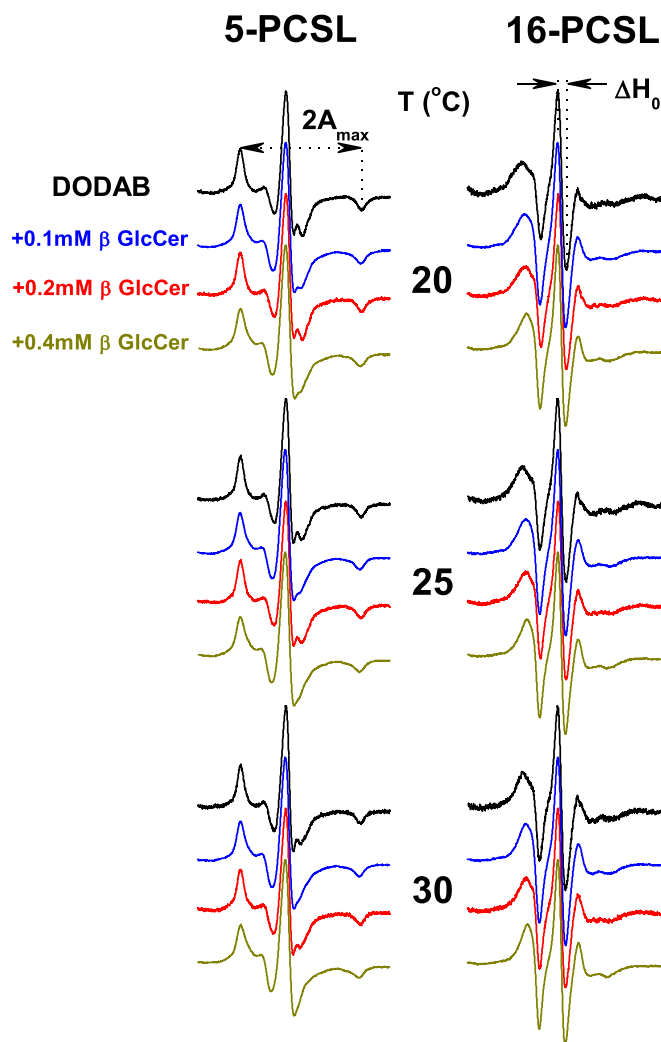

Fig. 3. Effect of βGlcCer on ESR spectra of 5-PCSL and 16-PCSL embedded in 2 mM DODAB bilayers at temperatures below the gel-fluid transition. The maximum hyperfine splitting (A_{max}) and the central field linewidth (ΔH_0) are indicated. Total spectra width is 100 G.

coexistence of rigid and fluid domains within the membranes [27,33] (Fig. 5).

At 40 °C, the spectra of 5- and 16-PCSL in pure DODAB membranes and in mixtures with 0.1 mM and 0.2 mM βGlcCer display two signals in the same spectrum, while the spectra for the mixture containing 0.4 mM βGlcCer are more isotropic and characteristic of a fluid phase (Fig. 5).

At 45 °C, the spectra of both probes still display two signals in pure DODAB bilayers, while in all mixed bilayers the spectra are characteristic of a fluid phase, indicating that the phase transition has been completed for all these mixed samples (Fig. 5). At 48 °C, the spectra of 5- and 16-PCSL are characteristic of the fluid phase for all membranes tested, indicating that the phase transition has also been completed for the pure DODAB bilayers (Fig. 5).

3.4. βGlcCer increases the DODAB fluid phase order and rigidity

Spectra of 5- and 16-PCSL in pure and mixed membranes are shown for the temperature range of 50 °C–60 °C in Fig. 6.

At this temperature range, the spectra of probes are typical of the fluid phase: 5-PCSL is in a fluid and ordered location (Fig. 6), close to the bilayer interface, where the labels have fast movement along their long axis [28]; 16-PCSL spectra indicate fast and nearly isotropic movement for the nitroxide radical at the bilayer core (Fig. 6), typical
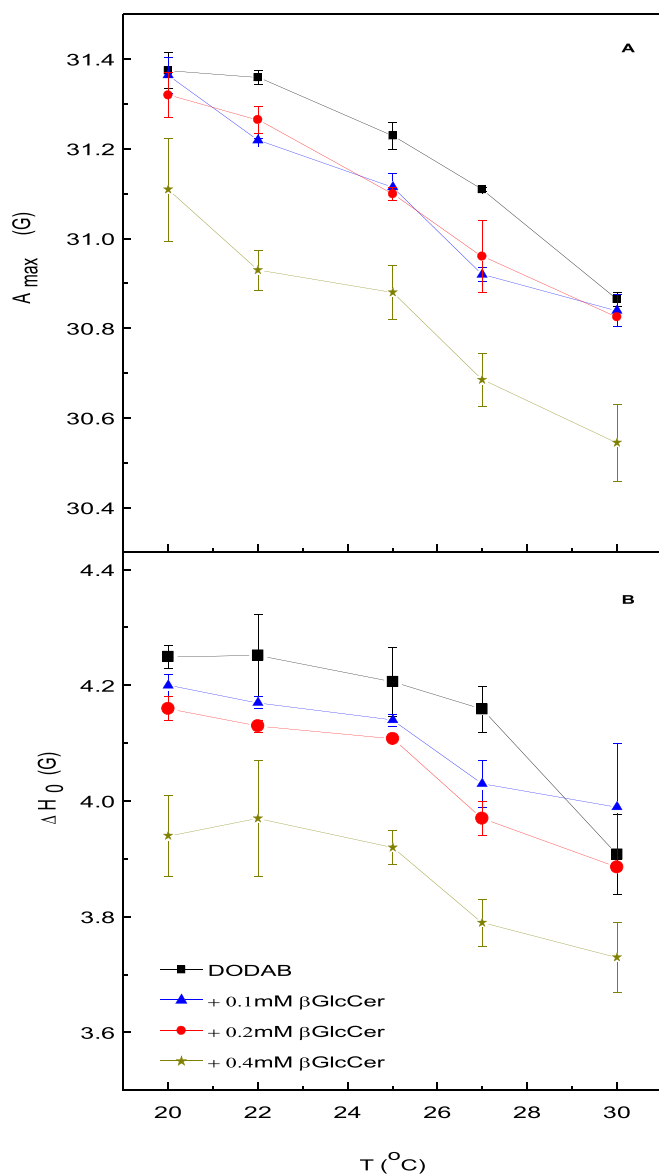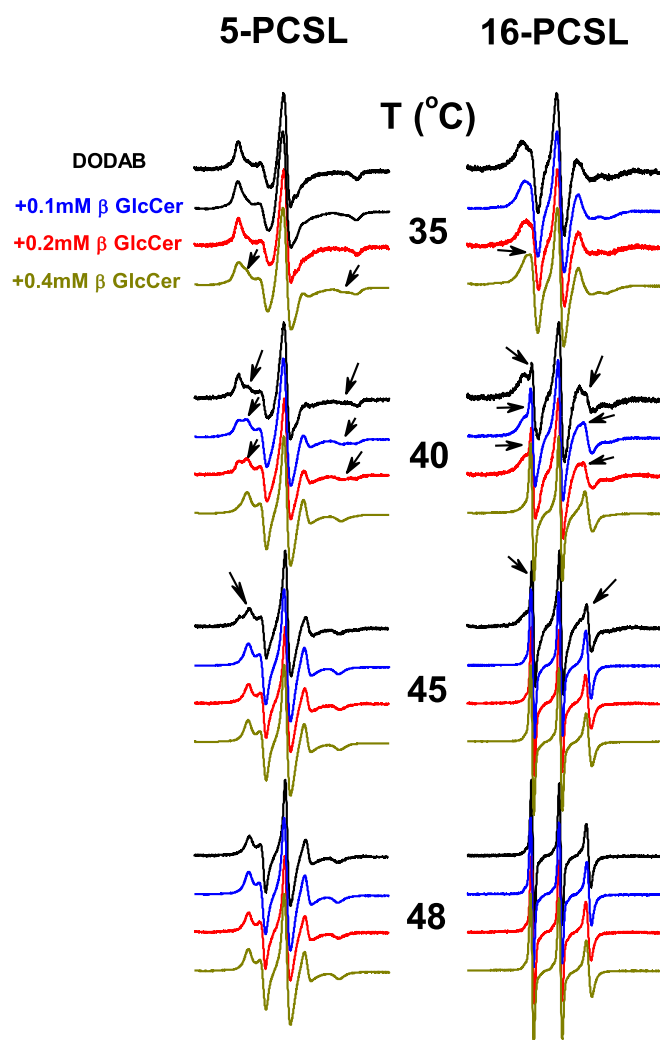
Fig. 4. Effect of βGlcCer on the maximum hyperfine splitting (A_{max}) of 5-PCSL (A) and on the central field linewidth (ΔH_0) of 16-PCSL (B) embedded in 2 mM DODAB bilayers at the gel phase.

Fig. 5. ESR spectra of 5-PCSL and 16-PCSL embedded in 2 mM DODAB or 2 mM DODAB + βGlcCer bilayers around the gel-fluid transition. Arrows indicate features of a more isotropic component which coexists with the typical gel phase signal.

of the motional narrowing region [28]. No obvious difference is observed on the spectra profile for both probes in the pure and mixed membranes (Fig. 6).

However, for the fluid phase, distinct parameters can be used to analyze the spectra of each spin label (Fig. 7). The effective order parameter (S_{eff}) is useful to evaluate acyl chain order with 5-PCSL (Fig. 7A). In this case, the position of the nitroxide group in an ordered environment, close to the bilayer surface, results in anisotropic ESR spectra with clearly defined maximum and minimum hyperfine splittings (A_{max} and A_{min}, respectively). These hyperfine splittings can be directly measured on the ESR spectra (Fig. 6) and are used to calculate the values of S_{eff} [34], as described in Section 2.4.

Mixed DODAB + βGlcCer membranes exhibit higher S_{eff} values than pure DODAB membranes (Fig. 7A), indicating that βGlcCer increases the bilayer order near the bilayer surface in the fluid phase.

Spin labels located deeper into the bilayer, such as 16-PCSL, sense a less ordered environment and yield more isotropic spectra, from which A_{max} and A_{min} cannot be measured. In this case, the ratio of the amplitudes of the high and central field lines (h_{-1} and h_0, as indicated in

Fig. 6) can be evaluated accurately. The h_{-1}/h_0 ratio decreases as the membrane viscosity increases [32].

The h_{-1}/h_0 values are smaller for mixed DODAB + βGlcCer membranes than for pure DODAB membranes (Fig. 7B), indicating that βGlcCer rigidifies the core of DODAB bilayers in the fluid phase.

3.5. No microscopic domains are observed in mixed DODAB + βGlcCer bilayers

DODAB bicelles have been used to solubilize hydrophobic drugs in their hydrophobic edges [27,35]. However, lipid miscibility in DODAB vesicles is dependent on molar fraction: DPPC below 30 mol%, for instance, was shown to demix from the cationic gel phase [36]. Since DODAB can spontaneously form giant vesicles (~10 μm) upon heating in aqueous solution [27], fluorescence microscopy was used to visualize if βGlcCer affects microscopic membrane homogeneity (Fig. 8).

DODAB and DODAB + 0.2 mM βGlcCer vesicles exhibit a typical faceted aspect in the gel phase (~25 °C) (Fig. 8 A and B), and a typical round shape in the fluid phase (~50 °C) (Fig. 8 C and D). The homogeneous surface fluorescence of pure and mixed liposomes suggests that there are no macroscopic domains (of size bigger than the optical resolution of about 0.4 μm) being formed by βGlcCer within the DODAB bilayers in both gel and fluid phases (Fig. 8 B and D). Since
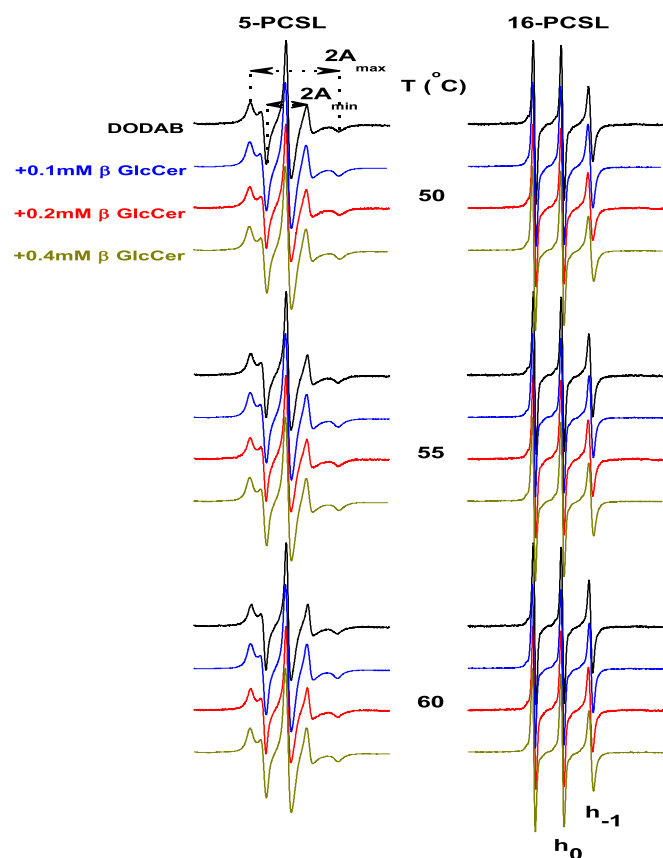
Fig. 6. Effect of βGlcCer on ESR spectra of 5-PCSL and 16-PCSL embedded in 2 mM DODAB bilayers at temperatures above the gel-fluid transition. Maximum and minimum hyperfine splittings (A_{max} and A_{min}) are indicated, as well as the positions of central (h_0) and high (h_{-1}) field lines. Total spectra width is 100 G.

photobleaching affects fluorescence images after long time observation (e.g. Fig. 8C), additional images of a large field of view are shown as Supplementary Material (Fig. S2). In addition, phase contrast images of the vesicles in Fig. 8 are shown along the heating process (Fig. S3).

4. Discussion

Pure C24:1 βGlcCer exhibits a complex thermotropic behavior, with peaks at 36 °C, 45 °C, 57 °C and 66 °C (Fig. 2). Such behavior was previously described for βGlcCer dispersions in water [31], and the small differences in peak positions are probably due to the much faster scan rate (30 °C/h) employed in the previous work. Following Björkvist and colleagues' interpretation [31], the most intense endothermic peak at 66 °C corresponds to the main gel-fluid phase transition, whereas the preceding peaks correspond to conversions between metastable gel phases that might differ in hydrocarbon packing organization, chain tilt, hydration of the headgroup or presence of interdigitation [37,38]. It is of note that ESR spectra of pure βGlcCer are characteristic of a non-interdigitated bilayer organization that undergoes a gel-to-fluid phase transition as temperature increases from 25 °C to 70 °C (see Supplementary Fig. S1).

The peaks observed in pure βGlcCer thermograms disappear in mixed bilayers, suggesting that βGlcCer is able to mix with DODAB at all fractions tested (Fig. 2). Moreover, the thermograms of all DODAB + βGlcCer bilayers present broad transitions shifted to smaller temperatures, indicating that βGlcCer induces a decrease in both the transition temperature and the cooperativity of the cationic bilayers (Fig. 2).

This is an unexpected result: since the gel-fluid temperature of βGlcCer is much higher than the one of DODAB, it would be likely that
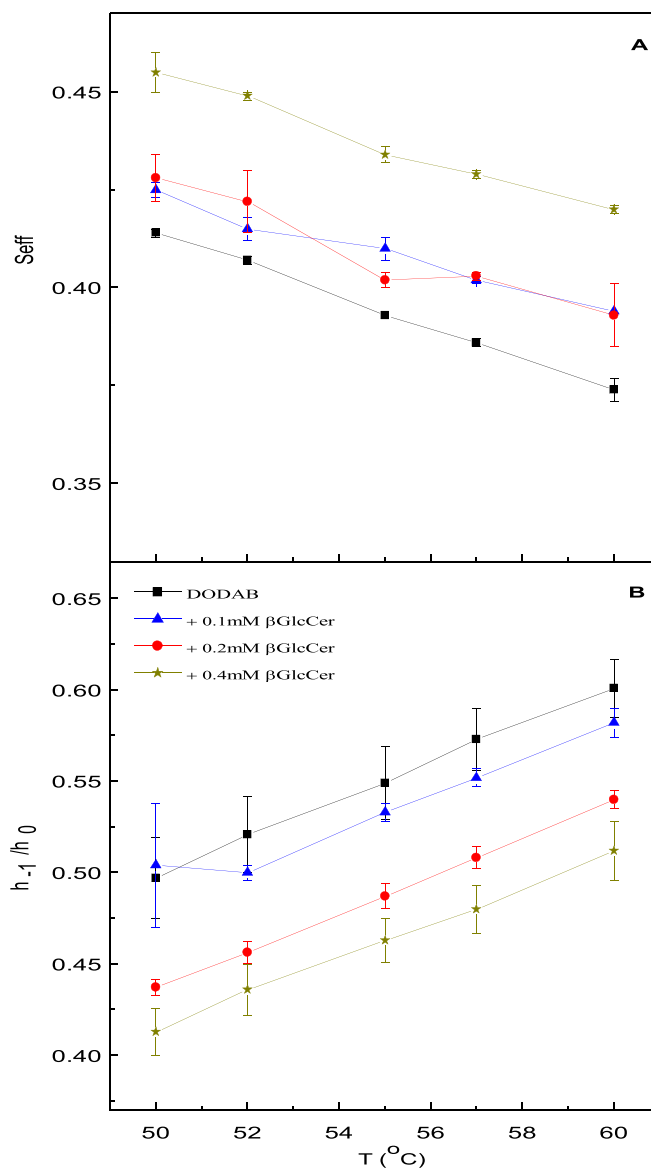
**Fig. 7.** Effect of mM βGlcCer on the effective order parameter (S_{eff}) from 5-PCSL spectra (A) and on h_{-1}/h_0 ratios from 16-PCSL spectra (B) embedded in 2 mM DODAB bilayers at the fluid phase.

this glucosylceramide would promote an increase in membrane order with a consequent increase in the melting temperature, as seen for mixtures of galactosylceramide and dimyristoylphosphatidylcholine [39]. On the other hand, it has been shown that monoolein (1-mono-oleoyl-*rac*-glycerol), a neutral unsaturated lysolipid, also decreases the transition temperature and cooperativity of DODAB bilayers [40]. This illustrates the dependence of phase transition thermodynamics on the structures of the lipids involved, and emphasizes the need of additional techniques to fully understand such complex phenomena.

Consistently, βGlcCer is able to destabilize the DODAB gel phase as seen from the decrease in bilayer packing at the core and near the surface represented by smaller A_{max} and ΔH_0 values (Fig. 4A and B). It is a consequence of the structural features of βGlcCer, which is composed of a glucosyl moiety and a ceramide moiety (Fig. 1).

The glucosyl moiety is bulky and able to make extensive hydrogen bonding through its hydroxyl groups (Fig. 1). Molecular simulations suggest that the glucosyl headgroup is more hydrated than its galactosyl isomer [41], implying that the glucosyl headgroup size would be further increased due to hydrogen bonding to water and that
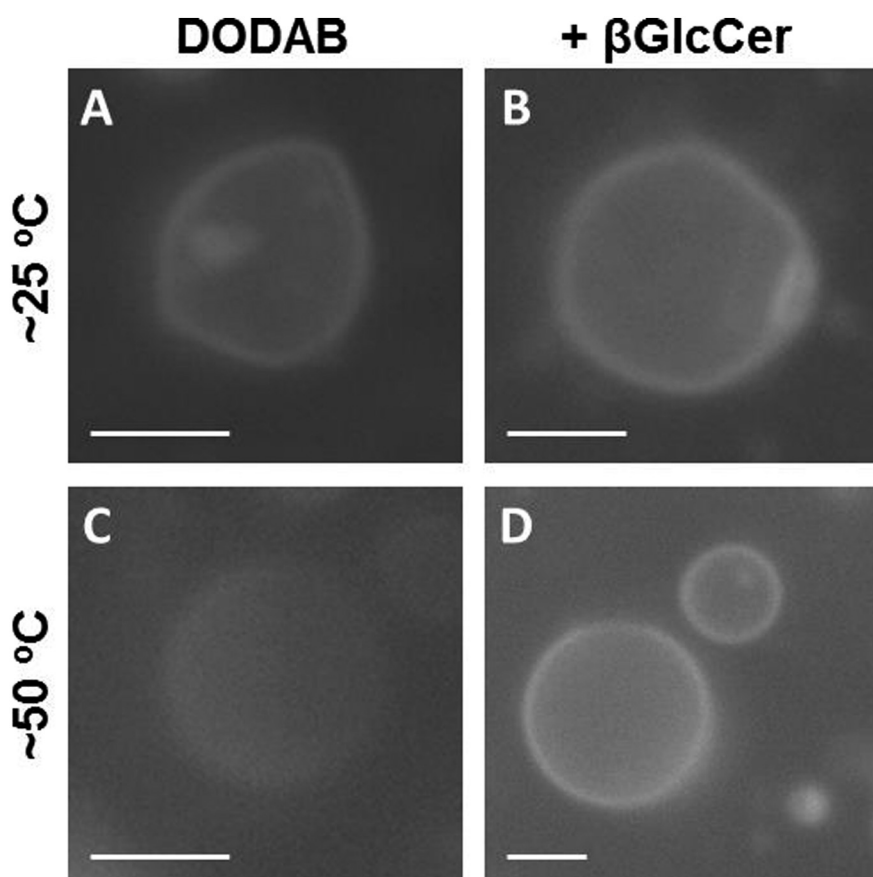
DODAB

+ βGlcCer

Fig. 8. Fluorescence microscopy (0.5 mol% PE-Rh) images of vesicles of 2 mM DODAB (A and C) and 2 mM DODAB + 0.2 mM βGlcCer (B and D) in the gel (A and B) and fluid (C and D) phases. The scale bar represents 4 μm. The image in C was obtained after long exposure of the vesicle to the illumination, which caused significant fluorescence photobleaching. The contrast of the snapshots was enhanced.

intermolecular interactions between the glycolipids would be decreased. This is in line with observations that although glucosyl headgroups have lower thermotropic stability than galactosyl groups, they increase the number of intermediate structures that the lipid can adopt [42]. The bulky and very hydrated glucosyl headgroup would have a larger space requirement than the small and poorly hydrated quaternary ammonium headgroup of DODAB [43], which would explain the superficial decrease in bilayer packing of the DODAB gel phase induced by βGlcCer (Fig. 4A). It is important to note that, despite being a cationic lipid, the repulsion between the DODAB quaternary ammonium headgroups is shielded by the HEPES buffer. Indeed, the phase transition temperature for DODAB bilayers in pure water is about 3 °C smaller than the ones in buffer [44], as expected from the larger electrostatic repulsion between charged headgroups in pure water.

The ceramide moiety of βGlcCer is made of a sphingoside base with a C4-*trans* double bond and a much larger C24 N-linked acyl chain with a 15-*cis* double bond (Fig. 1). The C4-*trans* bond promotes a vertical sphingoside chain orientation that facilitates a compact packing of ceramide chains [45,46], whereas the 15-*cis* bond disturbs acyl chain packing by increasing lateral space requirements, and decreasing chain order and interactions between polar groups [45,47]. In fact, the presence of the *cis* double bond lowers the transition temperature and affects the kinetics of formation of various metastable and stable gel phases of galactosylceramides [48] by precluding the formation of intermolecular hydrogen bonds [49]. This hindrance might affect not only the hydrogen bonding by the sugar moiety, but also by the amide-linked carbonyl group and the hydroxyl group of the ceramide moiety.

Monolayers of pure C24:1 ceramide or galactosylceramide at 22 °C were shown to have an axial displacement between the sphingoside and N-acyl chains, which places the kink caused by the 15-*cis* double bond above the end of the sphingoside chain [45,50]. In that case, the carbons placed above the end of the sphingoside chain would be able to penetrate the other monolayer and form transbilayer interdigitated gel

phases with an increased packing and a decreased degree of motion. However, the flexibility gradient toward the membrane core is not affected by βGlcCer (Fig. 3), as would be expected from an interdigitated gel phase [51,52], and the bilayer packing effectively decreases in presence of this glycolipid (Fig. 4A and B). Accordingly, it has been suggested that *cis* double bonds inhibit transbilayer lipid interdigitation under physiological conditions [48]. Hence, the evidence in the present work does not support the idea of an axial displacement of βGlcCer in the gel phase.

Although no significant differences in spectra profiles between pure and mixed bilayers are observed in the gel phase (Fig. 3), ESR spectra in some temperatures around the phase transition are the sum of anisotropic and isotropic signals, showing the coexistence of rigid and fluid lipid populations within the membranes in both pure and mixed bilayers (Fig. 5).

In pure DODAB bilayers, it is possible to observe the coexistence of rigid and fluid lipids at 40 °C, as previously described [33,53], and at 45 °C. At 48 °C, the pure bilayers display typical fluid phase spectra (Fig. 5). In presence of 0.1 mM and 0.2 mM βGlcCer, the coexistence of phases is even more evident at 40 °C, while the spectra for these mixed bilayers is already typical of fluid phases at 45 °C (Fig. 5). The earlier onset of phase transition is even more pronounced in presence of 0.4 mM βGlcCer: the coexistence of two phases is already observable at 35 °C, and at 40 °C the bilayer is already at the fluid phase (Fig. 5). This is consistent with the decrease in transition temperature induced by βGlcCer observed by DSC (Fig. 2).

In contrast to the decrease in bilayer packing of the gel phase, βGlcCer increases surface bilayer order and rigidifies the bilayer core of the DODAB fluid phase, as observed from higher S_{eff} and smaller h_{-1}/h_0 values (Fig. 7A and B). S_{eff} includes contributions from chain order and rate of motion, but the main contribution is the amplitude of acyl chains segmental motion [34]. The increase in surface bilayer order could be ascribed to an increase in hydration of the glucosyl headgroup

in the fluid phase, which would limit the amplitude of acyl chains segmental motion from neighboring DODAB molecules. Indeed, the number of water molecules associated with glycolipid headgroups in the fluid phase was shown to double when compared to the gel phase [54].

The decrease in h_{-1}/h_0 values in presence of βGlcCer (Fig. 7B) represent an increase in the viscosity of the bilayer core probed by 16-PCSL [32], possibly resulting from a more limited motion of DODAB acyl chains caused by the large and kinked acyl chain of βGlcCer. The increase in ordering and rigidity of the fluid phase could also arise from a movement of the spin label up, so that it would be probing a more ordered region. Although a vertical movement has been described for single chained spin labels [33], it is very unlikely that double tailed spin labels such as the ones employed in the present work would suffer from such an effect due to their stronger van der Waals and hydrophobic interactions. In fact, galactosylceramides that were themselves spin labeled also showed the capacity to increase rigidity in fluid lipid membranes [55].

It is noteworthy that a decrease in gel phase bilayer packing and an increase in fluid phase ordering were also observed for DODAB bilayers in the presence of cholesterol at fractions lower than 15 mol% [53]. Moreover, cholesterol has a low miscibility in DODAB [53], just as βGlcCer and other glycosphingolipids and ceramides have low miscibilities in fluid phase phospholipid membranes and tend to segregate into gel domains, macro ripple phases or even tubular structures [56].

This would suggest that lateral phase separation or the formation of domains could explain the similar effects of βGlcCer and cholesterol in DODAB bilayers. However, no microscopic domain or three-dimensional structure is observed in fluorescence microscopy images of DODAB bilayers containing βGlcCer (Fig. 8), which is in agreement with the disappearance of the peaks of pure βGlcCer in the thermogram of mixed bilayers (Fig. 2). Consistently, no nanoscopic domains are detected by ESR in mixed bilayers, because a single population is observed in the spectra of gel and fluid phases (Figs. 3 and 6). Since the spin labels can partition into pure βGlcCer bilayers (as seen in Supplementary Fig. S1), the absence of two populations is not an artifact due to probe exclusion from βGlcCer domains as previously observed with polymerizable lipids [57].

The physicochemical properties of liposomes play an important role in the development of novel immunotherapeutic tools: for instance, liposomes of greater rigidity and higher gel-fluid transition temperature elicit higher antibody and cell-mediated responses to antigens [58]. Hence, from the data presented in this paper, it is possible to assume that the formulation with the smallest fraction of βGlcCer (2 mM DODAB + 0.1 mM βGlcCer) would be the most efficient adjuvant in biological assays, since it has affected much less the phase transition of DODAB than the other fractions tested (Fig. 2). As a next step, it would be interesting to investigate the biological properties of these formulations.

To the best of our knowledge, this work is the first to characterize the structure of a glycosphingolipid embedded into a cationic bilayer, both in the gel and fluid phases. Mixed membranes employing these lipids may find important biological applications in developing areas such as immunotherapy [23,24].

5. Conclusions

The structure of cationic DODAB bilayers containing different amounts of unsaturated C24:1 β-glucosylceramide (βGlcCer) was investigated by means of DSC, ESR spectroscopy and fluorescence microscopy. βGlcCer is completely miscible within the DODAB bilayers at all fractions tested, since no domains were observed in fluorescence microscopy and ESR spectra. βGlcCer destabilized the gel phase of DODAB bilayers by decreasing the gel phase packing. As a consequence, it induced a decrease in the phase transition temperature and cooperativity of DODAB bilayers. βGlcCer also induced an increase in

DODAB fluid phase order and rigidity. A similar effect of loosening the gel phase packing and turning the fluid phase more rigid has been observed when low molar fractions of cholesterol were incorporated in DODAB bilayers. The structural characterization of mixed membranes made of cationic lipids and glucosylceramides may be important for planning novel biotechnology tools aimed at harnessing the biological effects of these lipids, as is the case of vaccine adjuvants.

Transparency document

The Transparency document associated with this article can be found, in online version.

Appendix A. Supplementary data

Supplementary data to this article can be found online at https://doi.org/10.1016/j.bbamem.2018.12.018.

References

[1] Y. Ishibashi, A. Kohyama-Koganeya, Y. Hirabayashi, New insights on glucosylated lipids: metabolism and functions, Biochim. Biophys. Acta Mol. Cell Biol. Lipids 1831 (2013) 1475–1485.

[2] G. D'Angelo, S. Capasso, L. Sticco, D. Russo, Glycosphingolipids: synthesis and functions, FEBS J. 280 (2013) 6338–6353.

[3] A.R. Todeschini, S. Hakomori, Functional role of glycosphingolipids and gangliosides in control of cell adhesion, motility, and growth, through glycosynaptic microdomains, Biochim. Biophys. Acta 1780 (2008) 421–433.

[4] G.A. Grabowski, Phenotype, diagnosis, and treatment of Gaucher's disease, Lancet 372 (2008) 1263–1271.

[5] E. Zigmond, S. Preston, O. Pappo, G. Lalazar, M. Margalit, Z. Shalev, L. Zolotarov, D. Friedman, R. Alper, Y. Ilan, β-Glucosylceramide: a novel method for enhancement of natural killer T lymphocyte plasticity in murine models of immune-mediated disorders, Gut 56 (2007) 82–89.

[6] W. Zhang, Y. Moritoki, K. Tsuneyama, G.X. Yang, Y. Ilan, Z.X. Lian, M.E. Gershwin, β-Glucosylceramide ameliorates liver inflammation in murine autoimmune cholangitis, Clin. Exp. Immunol. 157 (2009) 359–364.

[7] J.W.J. Hinrichs, K. Klappe, M. van Riezen, J.W. Kok, Drug resistance-associated changes in sphingolipids and ABC transporters occur in different regions of membrane domains, J. Lipid Res. 46 (2005) 2367–2376.

[8] M. Nagata, Y. Izumi, E. Ishikawa, R. Kiyotake, R. Doi, S. Iwai, Z. Omahdi, T. Yamaji, T. Miyamoto, T. Bamba, S. Yamasaki, Intracellular metabolite β-glucosylceramide is an endogenous Mincle ligand possessing immunostimulatory activity, Proc. Natl. Acad. Sci. U. S. A. 114 (2017) E3285–E3294.

[9] D.V. Lynch, M. Caffrey, J.L. Hogan, P.L. Steponkus, Calorimetric and X-ray diffraction studies of rye glucocerebroside mesomorphism, Biophys. J. 61 (1992) 1289–1300.

[10] W. Curatolo, Thermal behavior of fractionated and unfractionated bovine brain cerebrosides, Biochemistry 21 (1982) 1761–1764.

[11] D. Bach, I.R. Miller, Y. Barenholz, Thermotropic behavior of phosphatidylcholine-glucosylceramide mixtures: effects of phospholipid acyl chain composition and interaction with water, Biophys. Chem. 47 (1993) 77–86.

[12] Y. Feng, D. Rainteau, C. Chachaty, Z.W. Yu, C. Wolf, P.J. Quinn, Characterization of a quasicrystalline phase in codispersions of phosphatidylethanolamine and glucocerebroside, Biophys. J. 86 (2004) 2208–2217.

[13] D. Lu, D. Singh, M.R. Morrow, C.W.M. Grant, Effect of glycosphingolipid fatty acid chain length on behavior in unsaturated phosphatidylcholine bilayers: a ^{2}H NMR study, Biochemistry 32 (1993) 290–297.

[14] P.J. Quinn, The structure of complexes between phosphatidylethanolamine and glucosylceramide: a matrix for membrane rafts, Biochim. Biophys. Acta 1808 (2011) 2894–2904.

[15] H.J. Hinz, L. Six, K.P. Ruess, M. Lieflander, Head-group contributions to bilayer stability: monolayer and calorimetric studies on synthetic, stereochemically uniform glucolipids, Biochemistry 24 (1985) 806–813.

[16] K. Saxena, R.I. Duclos, P. Zimmermann, R.R. Schmidt, G.G. Shipley, Structure and

properties of totally synthetic galacto- and gluco-cerebrosides, J. Lipid Res. 40 (1999) 839–849.

[17] B. Maggio, M.L. Fanani, C.M. Rosetti, N. Wilke, Biophysics of sphingolipids II. Glycosphingolipids: an assortment of multiple structural information transducers at the membrane surface, Biochim. Biophys. Acta 1758 (2006) 1922–1944.

[18] C.T. Ilarduya, Y. Sun, N. Düzgünes, Gene delivery by lipoplexes and polyplexes, Eur. J. Pharm. Sci. 40 (2010) 159–170.

[19] C. Lonez, M. Vandenbranden, J.M. Ruysschaert, Cationic lipids activate intracellular signaling pathways, Adv. Drug Deliv. Rev. 64 (2014) 1749–1758.

[20] J.P. Neves Silva, A.C.N. Oliveira, M.P.P.A. Casal, A.C. Gomes, P.J.G. Coutinho, O.P. Coutinho, M.E.C.D. Real Oliveira, DODAB:monoolein-based lipoplexes as non-viral vectors for transfection of mammalian cells, Biochim. Biophys. Acta Biomembr. 1808 (2011) 2440–2449.

[21] J.H.K. Rozenfeld, S.R. Silva, P.A. Ranéia, E. Faquim-Mauro, A.M. Carmona-Ribeiro, Stable assemblies of cationic bilayer fragments and CpG oligonucleotide with enhanced immunoadjuvant activity *in vivo*, J. Control. Release 160 (2012) 367–373.

[22] L.R.M.M. Aps, M.B. Tavares, J.H.K. Rozenfeld, M.T. Lamy, L.C.S.F. Ferreira, M.O. Diniz, Bacterial spores as particulate carriers for *gene gun* delivery of plasmid DNA, J. Biotechnol. 228 (2016) 58–66.

[23] R.L. Coffman, A. Sher, R.A. Seder, Vaccine adjuvants: putting innate immunity to work, Immunity 33 (2010) 492–503.

[24] L.J. Carreño, S.S. Kharkwal, S.A. Porcelli, Optimizing NKT cell ligands as vaccine adjuvants, Immunotherapy 6 (2014) 309–320.

[25] J. Davidsen, I. Rosenkrands, D. Christensen, A. Vangala, D. Kirby, Y. Perrie, E.M. Agger, P. Andersen, Characterization of cationic liposomes based on dimethyldioctadecylammonium and synthetic cord factor from *M. tuberculosis* (trehalose 6,6′-dibehenate) – a novel adjuvant inducing both strong CMI and antibody responses, Biochim. Biophys. Acta 1718 (2005) 22–31.

[26] J.M. Boggs, G. Rangaraj, Phase transitions and fatty acid spin label behavior in interdigitated lipid phases induced by glycerol and polymixin, Biochim. Biophys. Acta 816 (1985) 221–233.

[27] J.H.K. Rozenfeld, E.L. Duarte, T.R. Oliveira, M.T. Lamy, Structural insights on biologically relevant cationic membranes by ESR spectroscopy, Biophys. Rev. 9 (2017) 633–647.

[28] W.L. Hubbel, H.M. McConnell, Molecular motion in spin-labeled phospholipids and membranes, J. Am. Chem. Soc. 93 (1971) 314–326.

[29] K.A. Riske, L.Q. Amaral, M.T. Lamy, Extensive perforation coupled with the phase transition region of an anionic phospholipid, Langmuir 25 (2009) 10083–10091.

[30] F.M. Linseisen, S. Bayerl, T.M. Bayerl, ^{2}H-NMR and DSC study of DPPC-DODAB mixtures, Chem. Phys. Lipids 83 (1996) 9–23.

[31] Y.J.E. Björkqvist, J. Brewer, L.A. Bagatolli, J.P. Slotte, B. Westerlund, Thermotropic behavior and lateral distribution of very long chain sphingolipids, Biochim. Biophys. Acta 1788 (2009) 1310–1320.

[32] D. Marsh, Experimental methods in spin-label spectral analysis, in: L.J. Berliner, J. Ruben (Eds.), Spin Labeling. Theory and Applications, Vol. 8 Plenum Press, New York, 1989, pp. 255–303.

[33] C.R. Benatti, E. Feitosa, R.M. Fernandez, M.T. Lamy-Freund, Structural and termal characterization of dioctadecyldimethylammonium bromide dispersions by spin labels, Chem. Phys. Lipids 111 (2001) 93–104.

[34] H. Schindler, J. Seelig, EPR spectra of spin labels in lipid bilayers, J. Chem. Phys. 59 (1973) 1841–1850.

[35] T.R. Oliveira, C.R. Benatti, M.T. Lamy, Structural characterization of the interaction of the polyene antibiotic amphotericin B with DODAB bicelles and vesicles, Biochim. Biophys. Acta 1808 (2011) 2629–2637.

[36] F.G. Wu, R.G. Wu, H.Y. Sun, Y.Z. Zheng, Z.W. Yu, Demixing and crystallization of DODAB in DPPC-DODAB binary mixtures, Phys. Chem. Chem. Phys. 16 (2014) 15307–15318.

[37] R.A. Reed, G.G. Shipley, Structure and metastability of N-lignocerylgalactosyl-sphingosine (cerebroside) bilayers, Biochim. Biophys. Acta 896 (1987) 153–164.

[38] P.R. Maulik, G.G. Shipley, X-ray diffraction and calorimetric study of N-lignocer-ylsphingomyelin membranes, Biophys. J. 69 (1995) 1909–1916.

[39] C. Linington, M.G. Rumsby, Galactosyl ceramides of the myelin sheath: thermal studies, Neurochem. Int. 3 (1981) 211–218.

[40] I.M.S.C. Oliveira, J.P.N. Silva, E. Feitosa, E.F. Marques, E.M.S. Castanheira, M.E.C.D. Real Oliveira, Aggregation behavior of aqueous dioctadecyldimethy-lammonium bromide/monoolein mixtures: a multitechnique investigation on the influence of composition and temperature, J. Colloid Interface Sci. 374 (2012) 206–217.

[41] T. Róg, I. Vattulainen, A. Bunker, M. Karttunen, Glycolipid membranes through atomistic simulations: effect of glucose and galactose head groups on lipid bilayer properties, J. Phys. Chem. B 111 (2007) 10146–10154.

[42] H.J. Hinz, H. Kuttenreich, R. Meyer, M. Renner, R. Fründ, Stereochemistry and size of sugar head groups determine structure and phase behavior of glycolipid membranes: densitometric, calorimetric, and X-ray studies, Biochemistry 30 (1991) 5125–5138.

[43] L. Woiterski, D.W. Britt, J.A. Käs, C. Selle, Oriented confined water induced by cationic lipids, Langmuir 28 (2012) 4712–4722.

[44] J. Cocquyt, U. Olsson, G. Olofsson, P. Van der Meeren, Thermal transitions of DODAB vesicular dispersions, Colloid Polym. Sci. 283 (2005) 1376–1381.

[45] H. Löfgren, I. Pascher, Molecular arrangements of sphingolipids. The monolayer behavior of ceramides, Chem. Phys. Lipids 20 (1977) 273–284.

[46] H.L. Brockman, M.M. Momsen, R.E. Brown, L. He, J. Chun, H.S. Byun, R. Bittman, The 4,5-double bond of ceramide regulates its dipole potential, elastic properties and packing behavior, Biophys. J. 87 (2004) 1722–1731.

[47] T. Maula, M.A. Al Sazzad, J.P. Slotte, Influence of hydroxylation, chain length, and chain unsaturation on bilayer properties of ceramides, Biophys. J. 109 (2015) 1639–1651.

[48] V.S. Kulkarni, R.E. Brown, Thermotropic behavior of galactosylceramides with *cis*-monoenoic fatty acyl chains, Biochim. Biophys. Acta 1372 (1998) 347–358.

[49] S. Ali, H.L. Brockman, R.E. Brown, Structural determinants of miscibility in surface films of galactosylceramide and phosphatidylcholine: effect of unsaturation in the galactosylceramide acyl chain, Biochemistry 30 (1991) 11198–11205.

[50] C. Stefaniu, A. Ries, O. Gutowski, U. Ruett, P.H. Seeberger, D.B. Werz, G. Brezesinski, Impact of structural differences in galactocerebrosides on the behavior of 2D monolayers, Langmuir 32 (2016) 2436–2444.

[51] J.M. Boggs, G. Rangaraj, A. Watts, Behavior of spin labels in a variety of interdigitated lipid bilayers, Biochim. Biophys. Acta 981 (1989) 243–253.

[52] J.H.K. Rozenfeld, E.L. Duarte, J.M. Ruysschaert, C. Lonez, M.T. Lamy, Structural characterization of novel cationic diC16-amidine bilayers: evidence for partial interdigitation, Biochim. Biophys. Acta Biomembr. 1848 (2015) 127–133.

[53] C.R. Benatti, R.M. Epand, M.T. Lamy, Low cholesterol solubility in DODAB liposomes, Chem. Phys. Lipids 145 (2007) 27–36.

[54] M. Köberl, H.J. Hinz, G. Rapp, Temperature scanning simultaneous small- and wide-angle X-ray scattering studies on glycolipid vesicles: areas, expansion coefficients and hydration, Chem. Phys. Lipids 91 (1998) 13–37.

[55] F.J. Sharom, C.W.M. Grant, Glycosphingolipids in membrane architecture, J. Supramol. Struct. 6 (1977) 249–258.

[56] A.R.P. Varela, A.M.P.S. Gonçalves da Silva, A. Fedorov, A.H. Futerman, M. Prieto, L.C. Silva, Effect of glucosylceramide on the biophysical properties of fluid membranes, Biochim. Biophys. Acta Biomembr. 1828 (2013) 1122–1130.

[57] C.F. Temprana, E.L. Duarte, M.C. Taira, M.T. Lamy, S. de Valle Alonso, Structural characterization of photopolymerizable binary liposomes containing diacetylenic and saturated phospholipids, Langmuir 26 (2010) 10084–10092.

[58] D.S. Watson, A.N. Endsley, L. Huang, Design considerations for liposomal vaccines: influence of formulation parameters on antibody and cell-mediated immune responses to liposome associated antigens, Vaccine 30 (2012) 2256–2272.